JACS
JOURNAL OF THE AMERICAN CHEMICAL SOCIETY
Article
pubs.acs.org/JACS

Structural and Biochemical Characterization of Organotin and Organolead Compounds Binding to the Organomercurial Lyase MerB Provide New Insights into Its Mechanism of Carbon−Metal Bond Cleavage

Haytham M. Wahba,[†,‡] Michael J. Stevenson,[§] Ahmed Mansour,[†] Jurgen Sygusch,[†] Dean E. Wilcox,[§] and James G. Omichinski*[,†]

[†]Département de Biochimie et Médicine Moléculaire, Université de Montréal, Montréal, Quebec H3C 3J7 Canada
[‡]Faculty of Pharmacy, Beni-suef University, Beni-suef, Egypt
[§]Department of Chemistry, Dartmouth College, Hanover, New Hampshire 03755, United States

Supporting Information

ABSTRACT: The organomercurial lyase MerB has the unique ability to cleave carbon−Hg bonds, and structural studies indicate that three residues in the active site (C96, D99, and C159 in *E. coli* MerB) play important roles in the carbon−Hg bond cleavage. However, the role of each residue in carbon−metal bond cleavage has not been well-defined. To do so, we have structurally and biophysically characterized the interaction of MerB with a series of organotin and organolead compounds. Studies with two known inhibitors of MerB, dimethyltin (DMT) and triethyltin (TET), reveal that they inhibit by different mechanisms. In both cases the initial binding is to D99, but DMT subsequently binds to C96, which induces a conformation change in the active site. In contrast, diethyltin (DET) is a substrate for MerB and the Sn^{IV} product remains bound in the active site in a coordination similar to that of Hg^{II} following cleavage of organomercurial compounds. The results with analogous organolead compounds are similar in that trimethyllead (TML) is not cleaved and binds only to D99, whereas diethyllead (DEL) is a substrate and the Pb^{IV} product remains bound in the active site. Binding and cleavage is an exothermic reaction, while binding to D99 has negligible net heat flow. These results show that initial binding of organometallic compounds to MerB occurs at D99 followed, in some cases, by cleavage and loss of the organic moieties and binding of the metal ion product to C96, D99, and C159. The N-terminus of MerA is able to extract the bound Pb^{VI} but not the bound Sn^{IV}. These results suggest that MerB could be utilized for bioremediation applications, but certain organolead and organotin compounds may present an obstacle by inhibiting the enzyme.

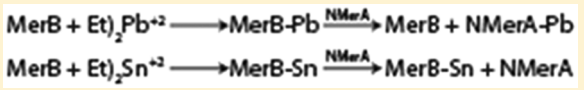

INTRODUCTION

Several strains of Gram-negative and Gram-positive bacteria have been isolated from mercury-contaminated sites because they possess the unique ability to grow in the presence of toxic concentrations of both inorganic mercury (Hg^{II}) and organomercurial compounds.[1] Their resistance to mercury-containing compounds is attributed to the presence of a set of genes located on a transferable genetic component known as the *mer* operon.[2−4] Although the exact composition of proteins produced from the *mer* operon varies among the different strains of resistant bacteria, the most common form of the operon encodes for proteins that function to detoxify both organomercurial compounds and ionic Hg^{II} by converting them to the less toxic elemental mercury (Hg^0).[5,6] The metabolic conversion of organomercurial compounds to Hg^0 requires two key enzymes encoded by the *mer* operon.[7−10] The first enzyme is the organomercurial lyase MerB, which cleaves the carbon−Hg bond of organomercurial compounds to produce a hydrocarbon and Hg^{II}.[7,8,11−13] The second enzyme is the ionic mercuric reductase MerA that uses NAD(P)H to reduce Hg^{II} to Hg^0, which is readily expired by the bacteria due to is volatility.[9,10]

When bacteria express both MerA and MerB, their mercury resistance is referred to as broad spectrum since they have the capacity to detoxify both Hg^{II} and organomercurial compounds.[6] Following exposure to ionic Hg^{II}, the toxic metal initially binds to two cysteine residues of the periplasmic protein MerP, which directly transfers the Hg^{II} to the mercury-specific transporter MerT.[14−16] This inner-membrane protein initially binds Hg^{II} with two cysteine residues located on the periplasmic side of the membrane followed by transfer to two cysteine residues located on the cytosolic side.[15] Once bound on the cytosolic side of MerT, the Hg^{II} is transferred directly to two cysteine residues within the amino-terminal domain of MerA (NMerA).[15,16] The NMerA-bound Hg^{II} is then transferred to two cysteine residues in the active site of MerA for NAD(P)H-dependent reduction to Hg^0.[17,18] In contrast to ionic Hg^{II}, organomercurial compounds pass directly into the cytosol due to their hydrophobicity, where they bind to MerB, which cleaves the carbon−Hg bond. Although X-ray structural studies have shown that the active site of MerB consists of three

Received: October 31, 2016
Published: December 17, 2016

DOI: 10.1021/jacs.6b11327
J. Am. Chem. Soc. 2017, 139, 910−921

key catalytic residues C96, D99, and C159 (*E. coli* MerB numbering), the mechanism of carbon−Hg bond cleavage by MerB is not well understood.[19,20] A current model suggests that one of the two cysteine residues initiates the reaction and D99 functions as a proton donor.[19,20] Following cleavage of the carbon−Hg bond, the resulting hydrocarbon is released, whereas the Hg^{II} product remains bound in the active site to C96, D99, and C159 until it is directly transferred to the two cysteine residues of NMerA.[13] As is the case following exposure to Hg^{II}, MerA reduces the Hg^{II} to Hg^0 as the final detoxification step of organomercurial compounds.[9,10] These direct transfers of Hg^{II} between the proteins in the Mer system, including between MerB and MerA, prevent the thiophilic Hg^{II} from binding to sulfhydryl groups of cellular proteins and thus limit its toxicity.

The unique catalytic property of MerB toward organomercurial compounds has attracted much attention for bioremediation applications in cleaning up mercury-contaminated sites, and several systems using either bacteria or plants expressing MerB and/or MerA have been developed as a form of green technology.[21−23] Unfortunately, organomercurial compounds represent only a small fraction of the organometallic compounds contaminating the environment. For example, organotin and organolead compounds pose serious threats to the environment.[24] Organotin compounds were commonly used as bactericides, fungicides, and stabilizers for polyvinyl chloride tubing, whereas organolead compounds were used extensively as antiknocking agents in gasoline for internal combustion engines.[25−28] As a result of the extensive use of tetraethyllead (TTEL) and tetramethyllead (TTML) as gasoline additives, tremendous quantities of organolead compounds were released in automobile exhaust[29] and these emissions remain an important source of organolead contamination in our environment. Likewise, tributyltin (TBT) and triphenyltin (TPT) were employed extensively in antifouling paints in the shipbuilding industry and this has contributed to the contamination of the marine environment, especially in harbors.[25,30]

Like organomercurial compounds, organolead and organotin compounds have the capacity to bioaccumulate and their concentrations are elevated in organisms that are higher on the food chain.[25] The toxicity of these compounds depends on both the type and number of organic groups bound to the metal, with higher substitution generally more toxic. The tetraalkyllead compounds TTEL and TTML are converted to their respective tri-, di-, and monoalkyl lead species, with the trialkylated lead species triethyllead (TEL) and trimethyllead (TML) the most persistent.[31,32] Following exposure, organolead compounds concentrate in the nervous system after crossing the blood−brain barrier, and the symptoms associated with exposure to organolead compounds include neurobehavioral abnormalities and impairment of memory.[33,34] In the case of organotin compounds, the toxic effects are associated in part with their direct impact on mitochondrial function. Trimethyltin (TMT) and triethyltin (TET) have been shown to inhibit mitochondrial oxidative phosphorylation, whereas diorganotin compounds where found to inhibit α-keto acid oxidase and consequently stop mitochondrial respiration.[35] For both organolead and organotin compounds, their toxicity is often associated with binding to sulfhydryl groups on proteins, as well as their capacity to bioaccumulate.

The toxic effects and widespread contamination of organotin and organolead compounds led several groups to investigate whether microorganisms have developed a natural resistant system similar to the Mer system used for organomercurial compounds.[32,36,37] Although select bacterial strains display resistance, a specific detoxification system, similar to the Mer system, has not been identified for either organolead or organotin compounds. To determine whether MerB possesses the capacity to cleave carbon−Sn bonds, a number of organotin compounds were tested[38] and it was determined that MerB has the capacity to cleave the C−Sn bond of several tetra- and trisubstituted derivatives. However, lower activity and a narrower range of specificity were found relative to its activity toward organomercurial compounds. Interestingly, a decrease in MerB catalytic activity with organotin compounds was noted as the reaction proceeded and carbon−Sn bond cleavage was observed. This suggested that the resulting di- or monosubstituted tin products might be inhibitors of MerB, and dimethyltin (DMT) was identified as a potent irreversible inhibitor.[38]

Given their similar properties and the fact that certain organotin compounds inhibit MerB, this suggests that organotin and organolead compounds could function as probes for characterizing the details of carbon−metal bond cleavage by MerB. Therefore, we have characterized the interaction of several organotin and organolead compounds with MerB using X-ray crystallography as well as isothermal titration calorimetry (ITC) and fluorescence spectroscopy measurements. Soaking crystals of MerB with solutions of organotin and organolead compounds revealed that initial binding to MerB occurs at D99, followed by cleavage and binding to C96 and C159 by some compounds. In addition, our results indicate that, like organotin compounds, organolead compounds appear to have the capacity to function as either substrates or inhibitors, depending on the chemical composition and the number of alkyl groups. Taken together, these results provide detailed insights into the catalytic mechanism of MerB for cleaving carbon−metal bonds and an atomic-level description of its interactions with organolead and organotin compounds.

MATERIALS AND METHODS

Expression Vector Construction, Expression, and Purification of MerB Enzyme. The *merB* gene from plasmid R831b cloned in pET21b expression vector (Novagen) was used for the expression of wild-type *E. coli* MerB. The sequences encoding the amino-terminal 69 residues of MerA (NMerA) from *Shigella flexneri* (UniProt code p08332) was cloned into a pGEX-TEV vector. All constructs were verified by DNA sequencing.

The *E. coli* MerB was expressed and purified as previously described.[19,39] During the purification, all buffers contained 1 mM ethylenediaminetetraacetic acid (EDTA) and 7.5 mM dithiolthreitol (DTT) to keep the cysteine residues in their reduced state. Following the purification, MerB samples were stored at −80 °C until further usage. Prior to crystallization, the protein samples were purified over a Superose-12 (GE Healthcare) gel filtration column using a buffer consisting of 10 mM sodium phosphate, pH 7.5, 1 mM EDTA, 10 mM sodium chloride, and 7.5 mM DTT (buffer A) and concentrated to 12 mg/mL using an Amicon ultrafiltration device with a 3 kDa MW cutoff (Millipore).

The GST-NMerA fusion protein was expressed in *E. coli* host strain TOPP2 (Stratagene). The cells were grown at 37 °C in Luria broth media, and protein expression was induced for 4 h at 30 °C with 0.7 mM isopropyl-β-D-thiogalactopyranoside (IPTG; Inalco). The cells were harvested by centrifugation, resuspended in lysis buffer (20 mM Tris·HCl pH 7.4, 1 M NaCl, 0.2 mM EDTA, and 1 mM DTT), lysed in a French press and centrifuged at 105000*g* for 1 h at 4 °C. The supernatant was then collected and incubated for 1 h with Glutathione

DOI: 10.1021/jacs.6b11327
J. Am. Chem. Soc. 2017, 139, 910−921

Table 1. Data Collection and Refinement Statistics for Organotin Compounds[a,b]

	MerB–DMT		MerB–DET, 1 h	MerB–TET, 1 h
	10 min	1 h		
PDB code	5U79	5U7A	5U7B	5U82
		Data Collection		
beamline	08ID-1, CLS	X25, NSLS-I	08-ID, CLS	08-ID, CLS
wavelength (Å)	0.9795 Å	1.100 Å	0.9724 Å	0.9724 Å
space group	$P2_1$	$P2_1$	$P2_1$	$P2_1$
unit-cell params (Å)	a = 38.58, b = 89.23, c = 54.68 α = 90, β = 98.48, γ = 90	a = 38.05, b = 88.64, c = 51.49 α = 90, β = 100.34, γ = 90	a = 37.86, b = 88.80, c = 55.01 α = 90, β = 97.19, γ = 90	a = 38.57, b = 88.93, c = 54.57 α = 90, β = 98.27, γ = 90
resolution (Å)	50.00–1.60 (1.66–1.60)	50.00–1.53 (1.58–1.53)	50–2.00 (2.07–2.00)	50.00–1.85 (1.91–1.85)
total reflections[b]	110 133	128 916	60 797	78 057
no. unique reflections	45 930	43 607	22 423	30 235
multiplicity	2.4	3.0	2.7	2.6
completeness (%)	95.94 (94.83)	86.48 (31.30)	92.00 (60.00)	97.00 (96.00)
R_{merge}	0.043 (0.45)	0.038 (0.47)	0.053 (0.38)	0.14 (0.76)
$I/\sigma(I)$	13.26 (2.50)	16.45 (1.61)	12.07 (2.25)	8.51 (1.57)
		Refinement Statistics		
resolution (Å)	50.00–1.60	50.00–1.53	50.00–2.00	50.00–1.85
R_{work}/R_{free} (%)	17.27/20.38	17.48/21.11	16.58/22.25	19.26/24.08
no. atoms (excluding hydrogens)				
protein	3190	3178	3181	3188
water	455	276	151	389
ligands	11	8	11	23
B-factors (Å^2)				
protein	25.80	27.90	42.70	24.79
water	37.60	33.90	41.30	32.67
ligands	24.70	21.10	25.70	20.48
metal occupancy	0.88/0.83	0.88/0.91	0.83/0.91	1.00/1.00
RMSDs				
bond length (Å)	0.011	0.011	0.013	0.011
bond angle (deg)	1.29	1.35	1.38	1.17
Ramachandran[c]				
favored (%)	97	95	95	97
outliers (%)	0.48	1.5	0	0

[a]Values in parentheses are for highest-resolution shell. $R_{sym} = \sum_{hkl}\sum_i |I_{hkl,i} - \langle I_{hkl}\rangle| / \sum_{hkl,i}\langle I_{hkl}\rangle$, where $I_{hkl,i}$ is the intensity of an individual measurement of the reflection with Miller indices hkl and I_{hkl} is the mean intensity of that reflection. $R_{work} = \sum_{hkl}\langle |F_o| - |F_c|\rangle / \sum_{hkl}|F_o|$, where $|F_o|$ is the observed structure-factor amplitude and $|F_c|$ is the calculated structure-factor amplitude. R_{free} is the R factor based on at least 500 test reflections that were excluded from the refinement. [b]Reflections with $F_o > 0$. [c]MolProbity analysis.

Sepharose 4B (GSH) resin (GE Healthcare) at 4 °C. Following incubation, the resin was collected by centrifugation, washed with lysis buffer, and placed in a TEV cutting buffer (25 mM sodium phsophate, 125 mM NaCl, and 5 mM DTT). The GST tag was cleaved by incubating the resin for 2 h with 100 units of TEV protease. The NMerA protein was eluted by two washes in TEV buffer. NMerA was further purified using High Performance Q-Sepharose (GE Healthcare) in 20 mM sodium phosphate buffer, pH 7.3, with 1 mM EDTA and 7.5 mM DTT (buffer B) and a Superdex 200 10/300 column (GE Healthcare) in buffer A. NMerA was flash-frozen and kept at −80 °C until being processed for fluorescence quenching experiments. For these experiments both MerB and NMerA were subjected to buffer exchange by passing through a Superdex 200 10/300 column (GE Healthcare) in 50 mM sodium phosphate buffer pH 7.4.

MerB Crystallization Conditions. Crystals of MerB were grown by the vapor diffusion method at 23 °C using either 1:1 or 1:2 mixtures of protein solution (12 mg/mL) and precipitant buffer, respectively. The precipitant buffer was 22–24% polyethylene glycol 2000 MME in 0.2 M sodium acetate, pH 5.5, with 0.2 M potassium bromide.

Formation of Metal and Organometal Complexes with MerB Crystals. To obtain MerB–organometal complexes, crystals of wild-type MerB were soaked for time periods ranging from 10 min to 6 h in a cryoprotectant solution containing 25% polyethylene glycol 2000 MME in 0.2 M sodium acetate, pH 5.5, with 0.2 M potassium bromide and 0.5–1.0 mM dimethyltin dibromide (DMT; Aldrich), diethyltin dichloride (DET; Alfa Aesar), trimethyltin chloride (TMT; Aldrich), diethyllead dibromide (DEL; Aldrich), trimethyllead bromide (TML; Aldrich), or triethyllead chloride (TEL; Crescent Chemicals). After soaking in the organometal solutions, the crystals were flash-cooled in liquid nitrogen for data collection.

X-ray Data Collection, Processing, and Structure Determination. Diffraction data were collected from single crystals using an ADSC Quantum 315 charge-coupled device at beamline X29 of the National Synchrotron Light Source (NSLS I) at Brookhaven National Laboratory (BNL, USA) or using a Rayonix MX300 detector at beamline 08ID-1 at the Canadian Light Source (CLS; Canada). All data sets were processed with HKL2000 or XDS, and the results are summarized in Tables 1 and 2. The initial phases for determining the structures of MerB following soaking with organometals were obtained by molecular replacement using the structure of wild-type MerB (PDB 3F0O) as a search template.[19,40] Phases were improved by iterative cycles of model building with Coot, and refinement was performed with Phenix.[41,42] Test data sets were randomly selected from the observed reflections prior to refinement. Statistics for the final models obtained with Phenix and Molprobity are shown in Tables 1 and 2.[43] The structure coordinates have been deposited in the RCSB Protein Data Bank. The figures were visualized using PYMOL.

Fluorescence Quenching Experiments. The binding of MeHg, DMT, DET, TET, DEL, and TML to MerB was monitored by

DOI: 10.1021/jacs.6b11327
J. Am. Chem. Soc. 2017, 139, 910–921

Table 2. Data Collection and Refinement Statistics for TML and DEL[a,b]

	MerB−TML, 10 min	MerB−DEL, 10 min
PDB code	5U88	5U7C
	Data Collection	
beamline	X25, NSLS-I	08-ID, CLS
wavelength (Å)	1.100 Å	0.9724 Å
space group	$P2_1$	$P2_1$
unit-cell params (Å)	a = 38.46, b = 88.78, c = 54.73	a = 38.06, b = 88.67, c = 54.83
	α = 90, β = 97.87, γ = 90	α = 90, β = 98.30, γ = 90
resolution (Å)	50.00−1.80 (1.86−1.80)	50−1.75 (2.81−1.75)
total reflections[b]	113 549	115 869
no. unique reflections	33 653	35 220
multiplicity	3.4	3.3
completeness (%)	99.77 (99.53)	97.00 (83.00)
R_{merge}	0.052 (0.81)	0.063 (0.67)
$I/\sigma(I)$	13.57 (1.62)	12.30 (1.91)
	Refinement Statistics	
resolution (Å)	50.00−1.80	50.00−1.75
R_{work}/R_{free} (%)	17.81/21.91	17.88/20.85
no. atoms (excluding hydrogens)		
protein	3190	3200
water	252	298
ligands	16	11
B-factors (Å^2)		
protein	37.30	31.81
water	41.50	40.60
ligands	45.80	22.74
metal occupancy (subunit A/B)	0.68/0.68	0.93/0.94
RMSDs		
bond length (Å)	0.011	0.010
bond angle (deg)	1.35	1.05
Ramachandran[c]		
favored (%)	95	96
outliers (%)	1.5	0.24

[a]Values in parentheses are for highest-resolution shell. $R_{sym} = \sum_{hkl}\sum_i |I_{hkl,i} - \langle I_{hkl}\rangle|/\sum_{hkl,i}\langle I_{hkl}\rangle$, where $I_{hkl,i}$ is the intensity of an individual measurement of the reflection with Miller indices hkl and I_{hkl} is the mean intensity of that reflection. $R_{work} = \sum_{hkl}\langle |F_o| - |F_c|\rangle/\sum_{hkl}|F_o|$, where $|F_o|$ is the observed structure-factor amplitude and $|F_c|$ is the calculated structure-factor amplitude. R_{free} is the R factor based on at least 500 test reflections that were excluded from the refinement. [b]Reflections with $F_o > 0$. [c]MolProbity analysis.

tryptophan fluorescence quenching with a Varian Cary Eclipse fluorescence spectrophotometer. For the fluorescence quenching experiments involving both MerB and NMerA, the proteins underwent buffer exchange by passing through a Superdex 200 10/300 column (GE Healthcare) in either 50 mM sodium phosphate buffer, pH 7.4 (MeHg, DEL, DET), or 50 mM Tris, pH 7.4 (DMT, TET, TML). A 1 mol equiv of Hg^{II}, DEL, or DET was added to 3.5−5 μM MerB at 25 °C. An excitation wavelength of 295 nm was used, and emission spectra in the 300−400 nm range were recorded before and after addition of the metal compounds. After formation of the organometal−MerB complex with MeHg, DET, and DEL, 20 mol equiv of NMerA (50 mM sodium phosphate, pH 7.4) was added and the spectrum was re-recorded.

Isothermal Titration Calorimetry (ITC) Experiments. Protein aliquots were stored in a −80 °C freezer until ITC preparation. All solutions were made and stored in acid-washed glass containers. Buffer solutions were made with nanopure water and treated with Chelex for at least 4 h before filtration to remove the Chelex resin. The metal-free buffers were then placed under vacuum (~5 Torr) with stirring for at least 2 h, or until no visible bubbles were being produced. The buffers were moved into an argon filled anaerobic environment in a CoyLab plexiglass glovebox and purged with argon through a gas diffuser for 10 min prior to sample preparation in the glovebox. MerB aliquots were buffer-exchanged using a PD-10 desalting column that had been equilibrated with 40 mL of the anaerobic buffer. The MerB protein concentration was determined using absorbance at 280 nm. Stock samples were prepared by dissolving the organometallic compound in buffer each day of experiments, and the working ITC samples were prepared from these in acid-washed glass vials. All ITC measurements were carried out in triplicate using either a MicroCal PEAQ-ITC, housed in a custom anaerobic plexiglass glovebox, with a 285 μL sample cell, a 40 μL titration syringe, 1.0−2.0 μL injection volumes, and 150−180 s intervals between injections, or a MicroCal VP-ITC, housed in a custom anaerobic plexiglass glovebox, with a 1.4 mL sample cell, a 300 μL titration syringe, 6−10 μL injection volumes, and 300−600 s intervals between injections.

RESULTS

Dimethyltin Binding to the Active Site of MerB. Although it has been shown that dimethyltin (DMT) is an irreversible inhibitor of MerB, the mechanistic details of this inhibition have not been investigated at the atomic level.[38] To characterize the mechanism of inhibition, crystals of MerB (*E. coli* MerB) were soaked for 10 min in a solution of 500 μM DMT, and the resulting crystals were found to diffract to 1.6 Å resolution with the same space group ($P2_1$) and the same number of proteins in the asymmetric unit (2) as crystals of free MerB (Table 1). The DMT-soaked crystals contain a tin atom bound in a trigonal bipyramidal geometry with 0.88 occupancy in a site that is 2.14 Å from an oxygen atom of D99

DOI: 10.1021/jacs.6b11327
J. Am. Chem. Soc. 2017, 139, 910−921

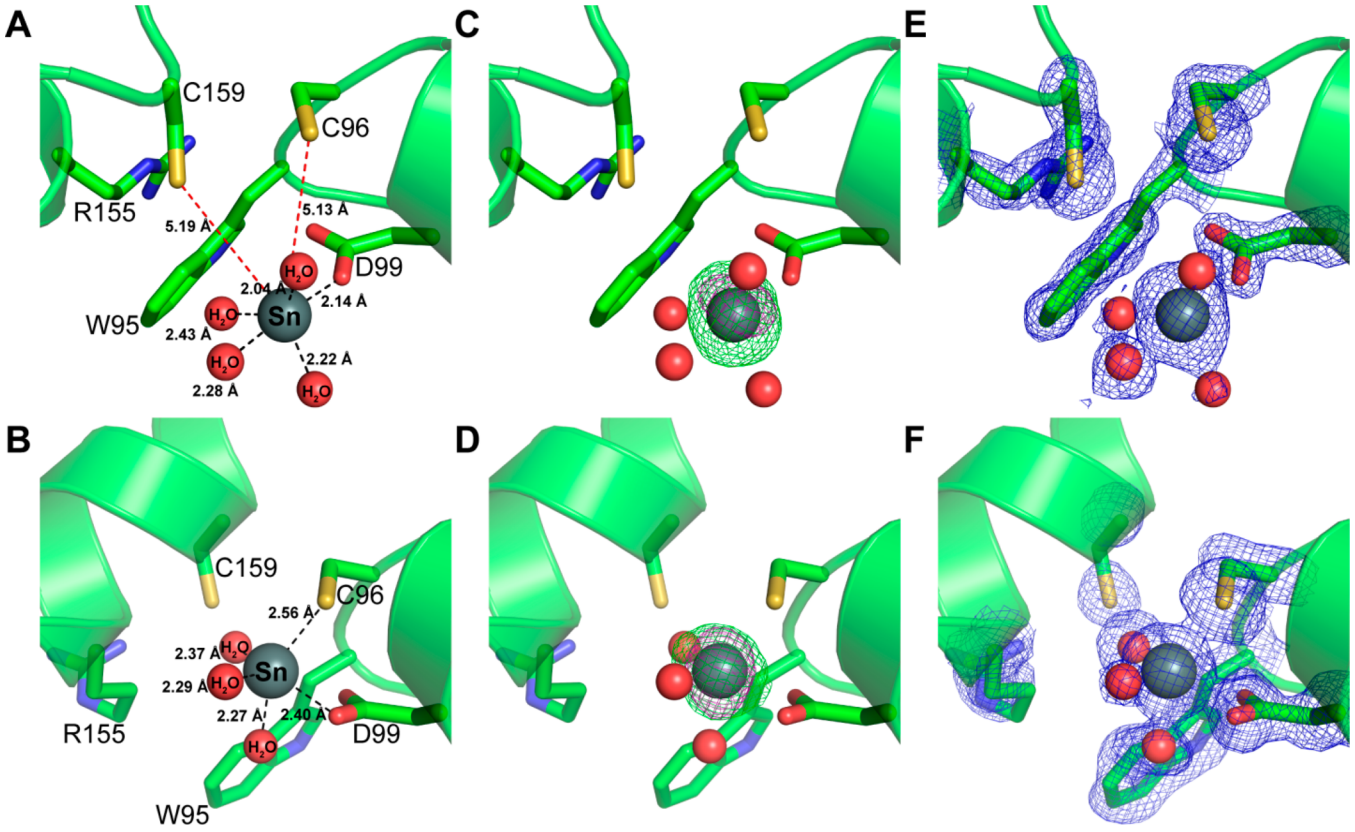

Figure 1. Comparison of the active site of the MerB–DMT complex (subunit A) after 10 min and 1 h. (A) Metrics of the MerB–DMT complex after 10 min soaking in DMT. The Sn atom (gray sphere) is bound to an oxygen of D99 (2.14 Å), and the oxygen atoms of four bound water (red sphere) molecules (2.04, 2.43, 2.28, 2.22 Å). The Sn atom is more distant to the sulfur atoms of C96 (5.13 Å) and C159 (5.19 Å). An important cation–π interaction between W95 and R155 in the active site is also highlighted. (B) Metrics of the MerB–DMT complex after 1 h soaking in DMT. The Sn atom (gray sphere) is bound to the sulfur of C96 (2.56 Å), an oxygen of D99 (2.40 Å), and the oxygen atoms of three bound water (red sphere) molecules (2.37, 2.29, 2.27 Å). Following the longer soak in DMT, the cation–π interaction between W95 and R155 is no longer present. (C, D) Close-ups of the F_o–F_c simulated annealing omit map contoured at 3σ displaying the positive density for the Sn atom (green mesh) and anomalous difference map showing the anomalous peak for the Sn atom (pink mesh) in the MerB–DMT complex after either a 10 min soak (C) or a 1 h soak (D) in DMT. The occupancies of the Sn atoms were set to zero prior to calculating the F_o–F_c simulated annealing omit map. (E, F) Close-ups of the F_o–F_c simulated annealing omit map contoured at 2.5σ (blue mesh) for the active site residues of the MerB–DMT complex after either a 10 min soak (E) or a 1 h soak (F) in DMT. The occupancies of C96, D99, and C159, as well as that of the Sn atom and bound water molecules, were set to zero prior to calculating the F_o–F_c simulated annealing omit map. Phenix map was used to generate the omit map calculation. The backbone of MerB is displayed in ribbon form (green), and the side chains of the three active site residues are displayed in stick form with the sulfur atoms (yellow) of C96 and C159 and the oxygen atoms (red) of D99.

(Figure 1A). In contrast to what is observed upon soaking MerB crystals with either an organomercurial substrate or $HgCl_2$, the tin atom does not bind to either cysteine residue in the active site, as it is located 5.13 Å from the sulfur atom of C96 and 5.19 Å from the sulfur atom of C159 (Figure 1A). Since methyl groups and bound water molecules generate similar electron density patterns, we were unable to determine whether either of the methyl groups of DMT was cleaved during formation of the complex with MerB. Attempts to refine the data with either one or two methyl groups on the tin atom did not provide the best difference maps, which could be attributed to multiple conformations of the methyl groups about the tin when it is bound to MerB. Therefore, water was used to model the other atoms coordinated to the tin atom in the refinement of the structure following soaking in a solution of DMT (Figure 1A).

Given the fact that a time lag in the inhibition of MerB following incubation with organotin compounds has been reported, MerB crystals were soaked in a DMT solution for longer time periods (up to 6 h) to determine if any changes occurred. Following a 1 h soaking in DMT, the resulting crystals diffract to 1.53 Å resolution with the same space group and two proteins in the asymmetric unit (Table 1). Consistent with results from the 10 min soak, analysis of subunit B from the asymmetric unit shows a tin atom binding with 0.88 occupancy to an oxygen atom of D99 of MerB (2.22 Å) and no interaction with the sulfur atom of either C96 (5.31 Å) or C159 (5.23 Å). However, analysis of subunit A from the asymmetric unit reveals that the tin atom is bound with 0.91 occupancy in a distorted trigonal bipyramidal conformation in contact with an oxygen atom of D99 (2.40 Å) and the sulfur atom of C96 (2.56 Å), but not the sulfur atom of C159 (5.83 Å) (Figure 1B). Interestingly, binding of the tin atom to D99 and C96 results in a dramatic change in the active site that disrupts a cation–π interaction between the guanidine group of R155 and the aromatic ring of W95 (Figure 1B). This interaction is present in the crystal structures of MerB in both the free and mercury-bound states, as well as in the structures after the 10 min soaking of DMT and in subunit B following the 1 h soaking (Figure 1). Disruption of this cation–π interaction between

DOI: 10.1021/jacs.6b11327
J. Am. Chem. Soc. 2017, 139, 910–921

R155 and W95 results in a conformational change in the H6 helix of MerB that displaces C159 away from the bound tin atom (Figure 1). This displacement of the C159 sulfur from the other two active site residues (2.35 Å further from the sulfur of C96 and 2.28 Å further from an oxygen of D99) helps to explain the irreversible inhibition of MerB by DMT.

Ethyl-Substituted Organotin Compounds Binding to MerB. To provide insight into whether the methyl groups are cleaved by MerB during formation of the complex following soaking in DMT, we solved the structure of MerB following soaking with diethyltin (DET) and triethyltin (TET). These compounds were selected because they are commercially available and sparingly soluble in aqueous solution, and the electron density of their ethyl side chains can be distinguished more readily from a bound water molecule than can methyl substituents. In addition, TET has also been reported to be an inhibitor of MerB, whereas DET is the closest commercially available analogue to DMT. Following soaking in 500 μM TET for 1 h, the resulting MerB crystals diffract to 1.85 Å resolution. The crystal structure reveals a MerB−TET complex with the tin atom bound at 1.0 occupancy to an oxygen atom of D99 (2.45 Å) in a trigonal bipyrimidal fashion and clear electron density for the three ethyl groups of TET, indicating that MerB does not cleave the carbon−Sn bonds. The tin atom in the MerB−TET complex does not bind the sulfur atom of either cysteine residue in the active site, as it is located 5.44 Å from the sulfur of C96 and 5.04 Å from the sulfur of C159 (Figure 2). Next, MerB crystals were soaked for 1 h in a solution containing 500 μM DET, and the resulting crystals diffract to 2.00 Å resolution. The crystal structure shows that the tin atom binds with 0.83 occupancy to an oxygen atom of D99 (2.10 Å) and the sulfur atoms of both C159 (2.39 Å) and C96 (2.57 Å) (Figure 3). In addition, there is no clear electron density for the two ethyl groups of DET, indicating that MerB has cleaved both carbon−tin bonds, and the Sn^{IV} remains bound at the active site, much like Hg^{II} remains bound upon MerB cleavage of MeHg.

Organolead Compounds Binding to MerB. The fact that organotin compounds have been shown to be substrates and/or inhibitors of MerB suggests that other organometallic compounds may have a similar interaction with the protein. Although many organometallic compounds react with oxygen or water, are unstable at room temperature, or are insoluble in aqueous solution, several organolead compounds are stable in aqueous solution at room temperature.[44,45] To investigate the interaction of organolead compounds with MerB, protein crystals were soaked for 10 min with a solution containing 500 μM trimethyllead (TML), which is readily soluble in aqueous solution, commercially available, and a persistent degradation product of TTML. Following the short soaking time, the resulting crystals diffract to 1.80 Å (Table 2). Analysis of the structure indicates that the lead atom binds to MerB with 0.68 occupancy, but that D99 is the only MerB residue that binds to the lead, which is 2.72 Å from an oxygen atom of D99, 5.52 Å from the sulfur atom of C96, and 5.12 Å from the sulfur atom of C159 (Figure 4 and see Figure S1 in Supporting Information). Soaking for longer time periods (up to 6 h) did not result in any change in the binding of the lead atom of TML, in contrast to what was found with DMT. However, we were able to determine that the methyl groups of TML are still present in the MerB−TML complex, which suggests that TML might be a weak inhibitor of MerB, like TET, which also binds to just D99.

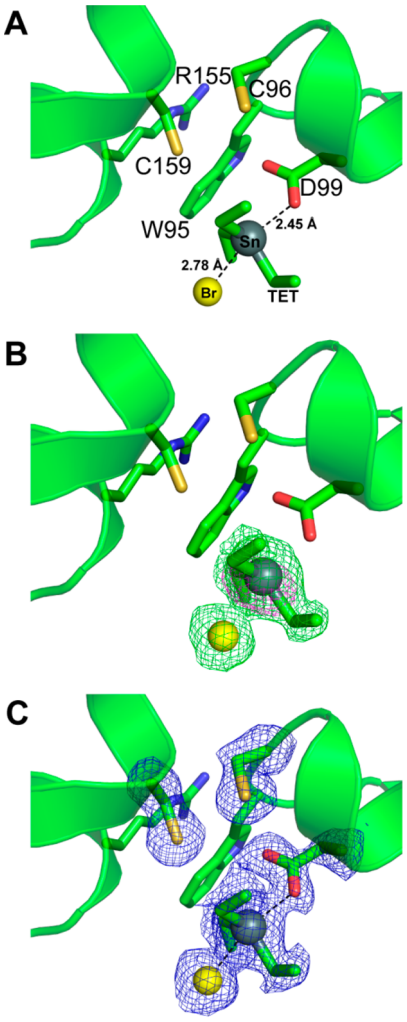

Figure 2. Binding of TET to the active site of the MerB (subunit A) after 1 h. (A) Metrics of the MerB−DMT complex after 1 h soaking in TET; the tin atom (gray sphere) is bound to an oxygen of D99 (2.45 Å) and a bromine atom (2.78 Å; yellow sphere). In this complex, the cation−π interaction is present between W95 and R155. (B) Close-up of the F_o−F_c simulated annealing omit map displaying the positive density for the TET atom (green mesh) and anomalous difference map showing the anomalous peak for the Sn atom (pink mesh) in the MerB−TET complex. The two maps are contoured at 3σ. The occupancy of TET was set to zero prior to calculating the F_o−F_c simulated annealing omit map. (C) Close up of the F_o−F_c simulated annealing omit map (blue mesh; contoured at 2.5σ) of the active site residues of the MerB−TET complex. The occupancies of C96, D99, C159, and the TET molecule were set to zero prior to calculating the F_o−F_c simulated annealing omit map. The Phenix map was used to generate the omit map calculation. The backbone of MerB is displayed in ribbon form (green), and the side chains of the three active site residues are displayed in stick form with the sulfur atoms (yellow) of C96 and C159 and the oxygen atoms (red) of D99.

To further investigate the interaction of organolead compounds with MerB, we examined diethyllead (DEL) binding to MerB. Like TML, DEL is readily soluble in aqueous solution, commercially available, and a persistent degradation product of TTEL. MerB crystals were soaked in a solution of 500 μM DEL, and the resulting crystals diffract to 1.75 Å (Table 2). In contrast to the MerB−TML complex, the crystal structure shows the lead atom binding with 0.93 occupancy to the sulfur atoms of both C96 (2.63 Å) and C159 (2.62 Å), as

DOI: 10.1021/jacs.6b11327
J. Am. Chem. Soc. 2017, 139, 910−921

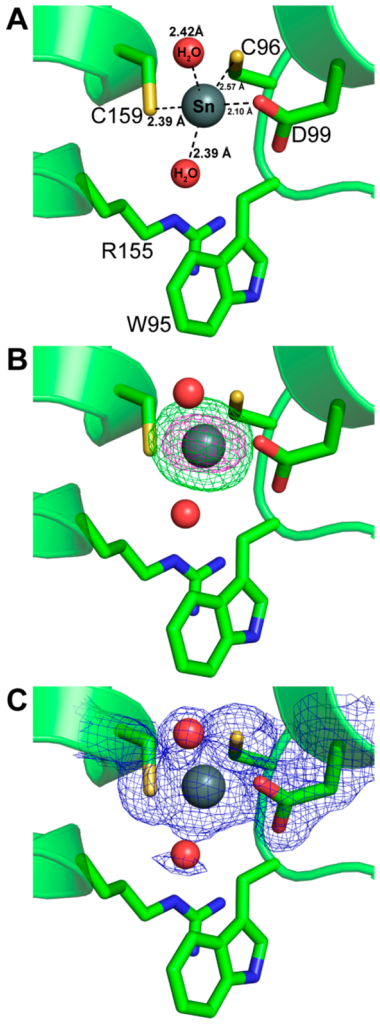

Figure 3. Binding of DET to the active site of the MerB (subunit A) after 1 h. (A) Metrics of the MerB−DET complex after 1 h soaking in DET; the tin atom (gray sphere) is bound to an oxygen of D99 (2.10 Å) and to the sulfur atoms of C96 (2.57 Å) and C159 (2.39 Å). In addition, the cation−π interaction between W95 and R155 is shown. (B) Close-up of the F_o-F_c simulated annealing omit map displaying the positive density for the Sn^{IV} atom (green mesh) and the anomalous difference map showing the anomalous peak for the Sn atom (pink mesh) in MerB−DET complex. The two maps are contoured at 3σ. The occupancy of Sn^{IV} was set to zero prior to calculating the F_o-F_c simulated annealing omit map. (C) Close-up of the F_o-F_c simulated annealing omit map (blue mesh; contoured at 2.5σ) of the active site residues of the MerB−DET complex. The occupancies of C96, D99, C159, and the Sn^{IV} and water molecule were set to zero prior to calculating the F_o-F_c simulated annealing omit map. The Phenix map was used to generate the omit map calculation. The backbone of MerB is displayed in ribbon form (green), and the side chains of the three active site residues are displayed in stick form with the sulfur atoms (yellow) of C96 and C159 and the oxygen atoms (red) of D99.

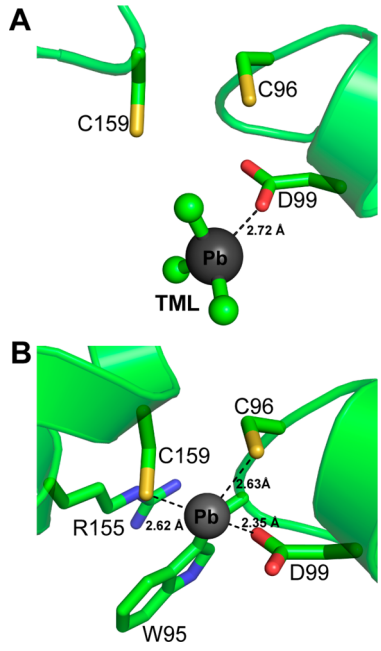

Figure 4. Binding of TML and DEL to the active site of the MerB. (A) Metrics of the MerB−TML complex (subunit B) after 10 min soaking in TML; the Pb atom (gray sphere) is bound to an oxygen of D99 (2.72 Å). (B) Metrics of the MerB−DEL complex (subunit A) after 10 min soaking in DEL; the Pb atom (gray sphere) is bound to an oxygen of D99 (2.35 Å) and to the sulfur atoms of C96 (2.63 Å) and C159 (2.62 Å). The backbone of MerB is displayed in ribbon form (green), and the side chains of the three active site residues are displayed in stick form with the sulfur atoms (yellow) of C96 and C159 and the oxygen atoms (red) of D99.

well as an oxygen atom of D99 (2.35 Å). Importantly, there is no electron density suggesting the presence of either of the ethyl groups, indicating that they have been cleaved, leaving the Pb^{IV} product bound to the active site of MerB and revealing that DEL is a substrate for MerB (Figure 4 and see Figure S1 in Supporting Information).

Fluorescence Measurements of Organotin and Organolead Compounds Binding to MerB. Given that the structural studies were performed with high concentrations of the organometallic compounds, we were interested in whether the organotin and organolead compounds, and especially DMT, TET, and TML, which are not substrates, bind to MerB at lower concentrations. Previous studies have shown that binding to the active site of MerB can be monitored experimentally by changes in the intrinsic fluorescence of the MerB tryptophan residues.[13] Addition of Hg^{II} reduces the MerB fluorescence in the 300−400 nm range, and this is attributed to a perturbation of the fluorescence of Trp95, which is located very close to the substrate binding site. As a control for using fluorescence to assess the binding of these organometallic compounds, we verified that addition of an organomercurial to MerB resulted in a change in the fluorescence. As observed with Hg^{II}, a significant quenching of the fluorescence signal occurs following the addition of 1 equiv of MeHg to a 5 μM solution of MerB (see Figure S2A in Supporting Information). Likewise, addition of 1 equiv of DMT, TMT, TET, TML, DET, or DEL to a 5 μM solution of MerB results in significant quenching of the MerB fluorescence (Figure 5 and see Figure S2B,C in Supporting Information). Due to competition by the buffer for the cationic organometallic compounds, these measurements provide only a qualitative indication of binding. However, the results show that all of the compounds, including DMT, TMT, TET, and TML that only coordinate to D99, have an appreciable affinity for MerB.

Calorimetric Measurements of Organotin and Organolead Compounds Binding to MerB. Since structural studies show that DMT, DET, TET, DEL, TML, and TMT

DOI: 10.1021/jacs.6b11327
J. Am. Chem. Soc. 2017, 139, 910−921

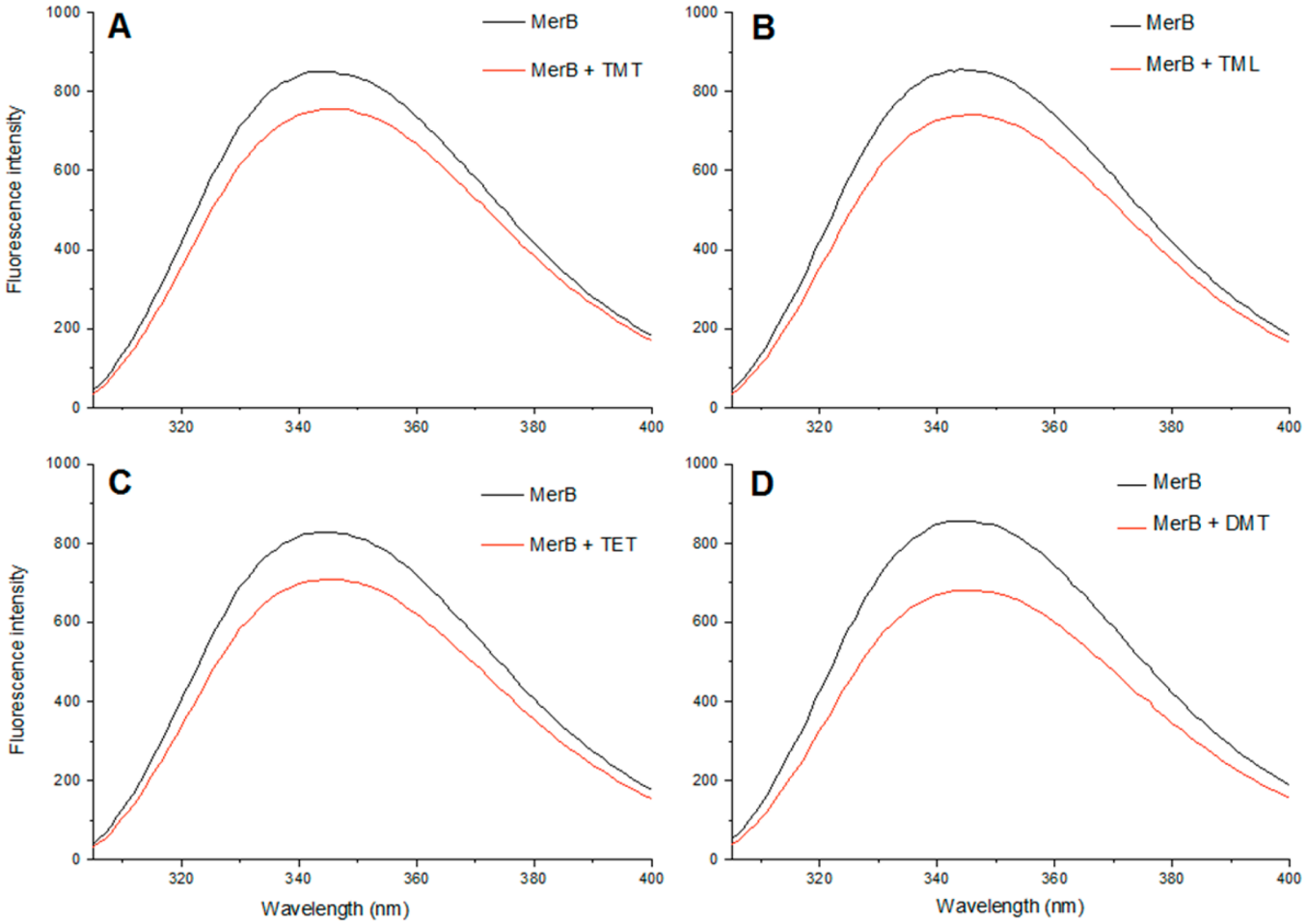

Figure 5. Organotin and organolead compounds bind MerB at low concentrations. The intrinsic fluorescence curve of MerB (5 μM) before (black line) and after (red line) the addition of 1 mol equiv of TMT (A), TML (B), DMT (C), or TET (D).

(trimethyltin; see Figure S3 and Table S1 in Supporting Information) all bind to the active site of MerB, though with differing coordination, we used isothermal titration calorimetry (ITC) to investigate their binding to MerB, with the aim of determining the thermodynamics of binding. ITC measurements were obtained for titrations of the organometallic compounds used in the crystal soaking experiments, as well as monomethyltin (MMT), into the MerB protein under anaerobic conditions. For some of these compounds, including MMT, TMT, and TML, there was no ITC evidence for an interaction with MerB in different buffers at pH 7.4. Since the crystal soaking experiments revealed that TML and TMT bind to the protein with metal coordination only to D99 and no cleavage of the alkyl groups, these ITC results suggest that this interaction is either too weak or has insufficient heat to be detected by a sensitive microcalorimeter. For other compounds, including DMT, DET, and DEL, there is a well-defined binding isotherm that can be fit to provide a stoichiometry and change in enthalpy for the interaction with the protein, as well as a "binding constant" (Figure 6). However, soaking experiments with these compounds revealed that the metal is coordinated to one or both of the Cys residues and there is an irreversible cleavage and loss of the organic fragment with DET and DEL. Since the binding of these compounds does not involve an equilibrium between free and bound compounds, an equilibrium constant cannot be determined from a fit of the isotherm. The ~1:1 stoichiometry found with this interaction reflects inhibition of MerB by the bound metal product and, in the case of DET and DEL, a single turnover. Table 3 indicates the experimental binding stoichiometry and enthalpy and the fit to a binding isotherm for those compounds with ITC evidence for an interaction with MerB, which are those with structural evidence for metal binding to the Cys thiols, but not those bound only to D99.

NMerA Extracts Pb^{IV} but Not Sn^{IV} from MerB–Pb^{IV} and MerB–Sn^{IV} Complexes. One of the important characteristics of the Mer system is the direct transfer of Hg^{II} between proteins until the final release of volatile Hg^0.[5] Maintaining the highly toxic Hg^{II} in a continuously bound state prevents it from binding to cellular proteins and interfering with their activity. In the case of MerB, the Hg^{II} product from cleavage of the carbon–Hg bond of organomercurials is transferred directly to NMerA. Previous studies have shown that this transfer of Hg^{II} from MerB to NMerA can be monitored by measuring changes in the fluorescence properties of MerB, as discussed above.[13] In these experiments, addition of Hg^{II} to MerB quenches its intrinsic fluorescence, and subsequent addition of excess NMerA to the MerB–Hg complex partially restores the fluorescence intensity upon removal of the bound Hg^{II} by NMerA.[13]

Given that both Sn^{IV} and Pb^{IV} are bound to MerB with a similar coordination as Hg^{II} following cleavage of the carbon–metal bonds of DET and DEL, respectively, we tested whether NMerA could remove either the bound Sn^{IV} or the bound Pb^{IV}.

DOI: 10.1021/jacs.6b11327
J. Am. Chem. Soc. 2017, 139, 910–921

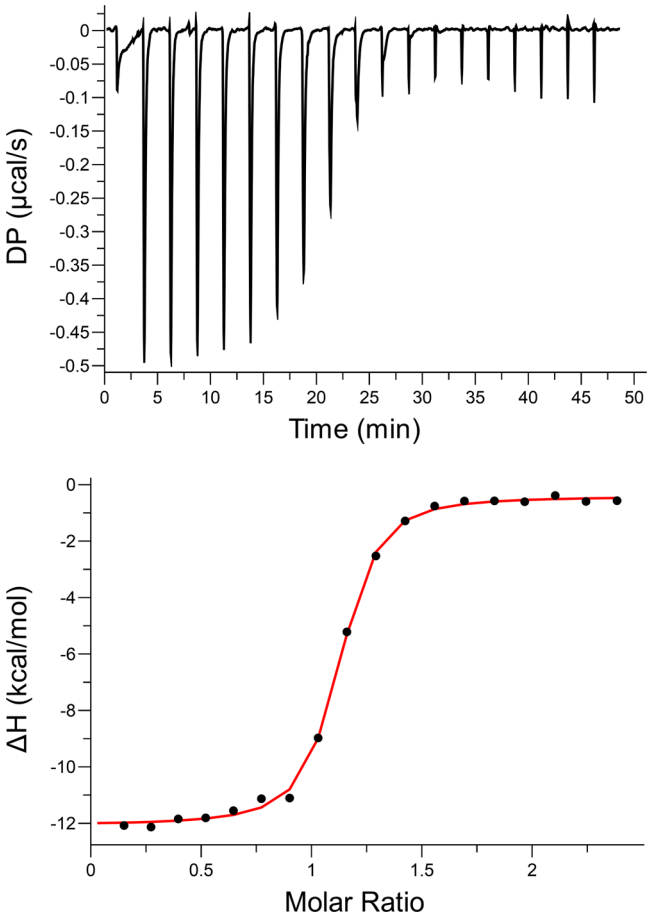

Figure 6. Representative ITC data for DEL titration into MerB, where 250 μM DEL was titrated into 20 μM MerB in 50 mM bisTris, pH 7.4, and 50 mM $NaNO_3$. The top panel shows the raw, baseline-smoothed ITC data plotted as heat flow versus time; the bottom panel shows the integrated concentration-normalized heat for each injection. The best-fit values with a nonlinear-least-squares analysis of the integrated data with PEAQ-ITC fitting software are n = 1.07 ± 0.04, K_{ITC} = 7.5 (±0.7) × 10^6, and ΔH_{ITC} = −11.6 ± 0.1 kcal mol^{-1}.

Table 3. Best Fit ITC Values with the One-Site Binding Model for Each Organometallic Compound Titrated into MerB

compound	buffer	n	K_{ITC}	ΔH_{ITC}[a]
DMT	Tris	0.9 ± 0.2	2 (±1) × 10^5	−6 ± 2
	PIPES	0.7 ± 0.1	5 (±4) × 10^5	−6.6 ± 0.5
DET	Tris	0.60 ± 0.05	4 (±1) × 10^6	−3.6 ± 0.3
	PIPES	0.57 ± 0.02	1.0 (±0.3) × 10^7	−6.7 ± 0.9
DEL	bisTris	1.0 ± 0.2	9 (±1) × 10^6	−12 ± 1

[a]In units of kcal mol^{-1}.

For these studies, the fluorescence signal of MerB was measured before and after the addition of 1 equiv of DET, DEL, or MeHg and a significant decrease in intensity was observed, indicating that the metals are bound in the active site of MerB (Figure 7). Following the addition of an excess of NMerA to the MerB−Pb^{IV} complex, a significant percentage of the fluorescence intensity of MerB was restored (~50% of the intensity loss following the addition of DEL at 344 nm; Figure 7A). In contrast, no significant change in the fluorescence intensity of MerB is observed following the addition of an excess of NMerA to the MerB−Sn^{IV} complex (Figure 7B).

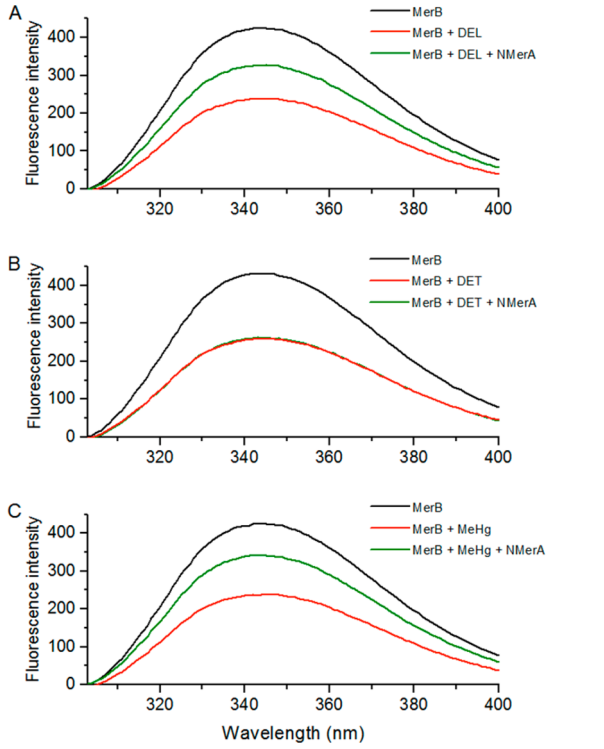

Figure 7. NMerA has the capacity to remove the bound lead from MerB. (A) Intrinsic fluorescence curve of MerB (5 μM) before (black line) and after (red line) the addition of 1 mol equiv of DEL. Following the addition of DEL, 20 mol equiv of NMerA (green line) was added to the MerB−Pb^{IV} complex. (B) Intrinsic fluorescence curve of MerB (5 μM) before (black line) and after (red line) the addition of 1 mol equiv DET. Following the addition of DET, 20 mol equiv of NMerA (green line) was added to the MerB−Sn^{IV} complex. (C) Intrinsic fluorescence curve of MerB (5 μM) before (black line) and after (red line) the addition of 1 mol equiv of MeHg. Following the addition of MeHg, 20 mol equiv of NMerA (green line) was added.

Likewise, no significant change in the fluorescence intensity of MerB is observed following the addition of an excess of NMerA to the MerB−TMT complex (see Figure S4 in Supporting Information), which indicates that NMerA is not able to remove the uncleaved organolead compound from MerB. These results suggest that NMerA is able to remove bound Pb^{IV}, but not bound Sn^{IV}, from the active site of MerB in a similar manner that it is able to remove bound Hg^{II} (Figure 7C).

DISCUSSION

MerB is one of two key enzymes involved in bacterial resistance to mercury due to its unique ability to cleave the carbon−Hg bond of a wide range of organomercurial compounds, including the natural environmental toxin MeHg.[5] Although mechanisms have been proposed for carbon−Hg bond cleavage by the three highly conserved residues in the MerB active site (C96, D99, and C159 in *E. coli* MerB),[19,20] the details of the cleavage reaction remain poorly understood. To further elucidate the roles of C96, D99, and C159 in carbon−metal bond cleavage, we have structurally and biophysically characterized the interaction of MerB with several organotin and organolead compounds, chosen because they are chemically similar to organomercurials, they are known environmental toxins, and

DOI: 10.1021/jacs.6b11327
J. Am. Chem. Soc. 2017, 139, 910−921

certain organotin compounds have been shown to be either inhibitors or substrates, of MerB.[38]

X-ray crystallography, complemented with fluorescence and ITC measurements, has revealed metric details and biophysical properties of organotin and organolead compounds binding to MerB. Starting with the previously identified organotin inhibitors DMT and TET and including the additional organotin compounds MMT, DET, and TMT, three types of binding to MerB were found. Both TET and TMT, as well as DMT initially, bind to D99 in the active site with no carbon−tin cleavage and, as shown for the trialkyl compounds, negligible binding enthalpy, suggesting a weak interaction associated with reversible inhibition of MerB. In the case of DMT, initial binding to D99 is followed by a shift to a coordination that also includes C96 and a structural rearrangement that displaces C159 and disrupts a cation−π interaction between W95 and R155 in the active site. This is associated with an exothermic binding enthalpy and irreversible DMT inhibition of MerB. Finally, DET binding results in an exothermic cleavage of both ethyl ligands and the resulting Sn^{IV} product remains coordinated to C96, D99, and C159 in a coordination similar to that of the Hg^{II} product following cleavage of organomercurial compounds. Of mechanistic relevance, there is no evidence that the monoalkyl compound MMT binds to MerB, even with the high concentrations used in crystal soaking.

Structural studies and biophysical measurements with the organolead compounds DEL and TML yield similar results as found with the analogous organotin compounds. TML binds only to D99 with negligible binding enthalpy, and DEL binds with cleavage of the two C96 bonds and the Pb^{IV} product remains coordinated to C96, D99, and C159 in an exothermic process. Finally, since the structural studies have revealed a Sn^{IV} or Pb^{IV} ion bound at the MerB site after carbon−metal bond cleavage with some compounds (DET, DEL), we show that NMerA is able to remove the Pb^{IV} product, but not the Sn^{IV} product, from the active site of MerB, much as it removes the Hg^{II} product after organomercurial cleavage.

These results clearly demonstrate that the initial binding of organotin and organolead compounds to MerB occurs at D99 and, for certain molecules, subsequent binding to C96 and C159 accompanies cleavage of the organometallic bonds and loss of the organic substituents as methane or ethane. These observations are somewhat surprising, given that all previous models for the mechanism of carbon−Hg bond cleavage by MerB postulated that the sulfhydryl of either C96 or C159 initiates the catalytic process, and the mechanistic debate has centered around which cysteine binds first. An initial binding role for D99 is also consistent with electrostatic attraction between the negatively charged carboxylate and the positively charged organometallic compounds, an interaction that has negligible net heat flow (binding enthalpy) and, therefore, is expected to be weak.

The residues corresponding to C96, D99, and C159 in *E. coli* MerB are conserved in all MerB proteins expressed from a wide range of bacterial strains, except for four cases.[46] In these four strains, the bacteria express two MerB proteins from their *mer* operon. The first, designated MerB1, contains the three catalytic residues corresponding to C96, D99, and C159 in *E. coli* MerB, but the second, designated MerB2, contains a serine residue in the position of the aspartic acid residue (D99), in addition to the two cysteine residues. (The four MerB2 proteins that contain the active site serine share 100% sequence identity.) Interestingly, the serine-containing MerB2 protein from *Bacillus megaterium* is considerably less efficient at cleaving carbon−Hg bonds relative to its MerB1 protein, which has an aspartic acid residue in the active site.[47−49] Finally, substituting serine in place of D99 in *E. coli* MerB results in a mutant protein that sequesters Cu^{II} when expressed in bacteria and has significantly lower catalytic activity.[50] Taken together with our current results on organotin and organolead compounds, initial binding to D99 is important not only for the catalytic activity of MerB, but also for metal selectivity.

The results obtained with this set of organotin and organolead compounds provide additional mechanistic insight about the catalytic activity of MerB. For these compounds, there is a clear reactivity (cleavage) preference for two organic groups (DET, DEL) over one (MMT) and three (TMT, TML). Further, there is a preference for those with ethyl substituents over those with methyl substituents. The balance between the number and type of groups on the organometallic substrate is reflected in the fact that DMT has a unique interaction with MerB (binding to Cys96 and D99 in the A subunit after a 1 h soak), yet DET is a substrate, even though both have two organic groups. Attempts to include additional organotin and organolead compounds in this study were limited by several factors, including low aqueous solubility with longer alkyl groups (e.g., dipropyl and dibutyl compounds), and the destruction of crystals following even short soaks with certain organometallic compounds. However, it is clear that the number and type of substituents attached to the metal dramatically alter the ability of MerB to bind and to cleave both organotin and organolead compounds.

Although Table 3 only contains condition-dependent enthalpies, the thermodynamics of the MerB cleavage reaction can be estimated. Formally this involves four steps: heterolytic carbon−metal bond cleavage, Cys thiol deprotonation, protonation of the formal carbanion, and metal binding to the Cys thiolate. The first two steps are endothermic, and the last two would be exothermic. The second and fourth steps may approximately cancel out, but the third step (protonation of a methyl or ethyl carbanion) is expected to be very exothermic. This step likely drives the reaction enthalpically, and loss of the resulting hydrocarbon drives it entropically. Of course these are formal steps and the cleavage reaction likely involves a concerted process. However, this parsing into formal steps allows some estimates for a heat inventory to explain the exothermic cleavage reaction of MerB.

The previously reported inhibition of MerB by organotin compounds has been structurally and biophysically elucidated in this study, which has included analogous organolead compounds. Reversible competitive inhibition is associated with coordination to the mechanistically important gatekeeper residue D99. Irreversible inhibition is associated with the unique coordination and rearrangement found with DMT and with those organotin compounds (DET), and presumably organolead compounds (DEL), that are cleaved by MerB and result in metal coordination to both active site cysteine residues. Finally, both the crystal structures and ITC measurements of those organometallic compounds that are cleaved show evidence for product (Sn^{IV} or Pb^{IV}) inhibition, as the metal remains bound after the crystal has soaked for 1 h in a large excess of the compound and the exothermic heat associated with binding and cleavage is only found up to ~1:1 stoichiometry. The observation that organolead compounds serve as substrates, and possibly inhibitors, of MerB,

DOI: 10.1021/jacs.6b11327
J. Am. Chem. Soc. 2017, 139, 910−921

depending on the number and type of substituents attached to the metal, is similar to the previously reported properties of certain organotin compounds.[38]

Although MerB evolved to cleave the methyl−mercury bond of the naturally occurring MeHg, its ability to cleave certain organotin and organolead compounds provides insight about the promiscuity and mechanistic requirements of this enzyme site. Of relevance is the strength of the carbon−metal bond that must be broken and the metal−thiolate bond that is formed. The Hg^{II} of organomercurial compounds has a lower charge density than Sn^{IV} and Pb^{IV} of the organotin and organolead compounds, and as a result, the native substrate has a higher thiophilicity (lower Lewis acidity) and forms stronger metal−thiolate bonds. However, the number, and to a lesser extent identity, of alkyl substituents on the Sn^{IV} and Pb^{IV} compounds will modulate their chemical properties, including the carbon−metal bond strength, and results in compounds with MerB reactivity similar to that of organomercurials. The match between the number of active site thiols and alkyl groups of the cleaved organotin and organolead compounds suggests a favorable correspondence between thiol proton donors and organic proton acceptors in the cleavage reaction. Clearly Sn^{IV} and Pb^{IV} are sufficiently thiophilic to remain tightly bound to C96, D99, and C159 in the MerB active site, which evolved to bind Hg^{II}.

Since MerB is able to cleave the carbon−metal bonds of certain organotin and organolead compounds, it may have the capacity to degrade these compounds, either naturally in bacterial strains containing the *mer* operon or when MerB is employed as part of a bioremediation system. However, to efficiently degrade these compounds, bacteria must be able to remove the resulting metal product from the MerB active site following cleavage of the carbon−metal bond(s). Our results indicate that NMerA has the ability to remove Pb^{IV}, but not Sn^{IV}, efficiently from MerB. Despite these results, it is not known whether MerA has the ability to reduce the Pb^{IV} once it has transferred from MerB, and it is not clear whether reducing the Pb^{IV} would be helpful to bacterial survival. Reducing Hg^{II} to Hg^0 leads to a volatile metal that is readily expired from the bacterium. Two-electron reduction of Pb^{IV} would produce Pb^{II}, which is still highly toxic. Further reduction to Pb^0 may provide some benefit since other studies have shown that converting Cu to Cu^0 provides some protection in bacteria.[51] However, Pb^0 is a solid and not a volatile liquid, like Hg^0. Therefore, it would probably be more beneficial for bacteria to transport the Pb^{II} directly out of the cell using a divalent metal transporter. In addition, organotin and organolead compounds may competitively inhibit the degradation of organomercurial compounds by MerB if they are jointly present as contaminants. Taken together, these results suggest that MerB could have a potential role in the degradation of both organotin and organolead compounds. However, it will be important for future studies attempting to use the *mer* system for bioremediation of organometallic compounds to consider the impact of the specific compounds that are present.

Abbreviations. *B. megaterium*, *Bacillus megaterium*; DEL, diethyllead(IV) dication; DET, diethyltin(IV) dication; DMT, dimethyltin(IV) dication; DTT, dithiothreitol; *E. coli*, *Escherichia coli*; EDTA, ethylenediaminetetraacetic acid; IPTG, isopropyl β-D-1-thiogalactopyranoside; ITC, isothermal titration calorimetry; LB, Luria−Bertani broth; MeHg, methylmercury(II) cation; MerA, organomercurial reductase from *mer* operon; MerB, organomercurial lyase from *mer* operon; MerB2, organomercurial lyase 2 from *mer* operon; MerP, periplasmic mercury transporter from *mer* operon; MerR, regulator for *mer* operon; MerT, mercury transporter from *mer* operon; MMT, monomethyltin(IV) trication; NMerA, amino-terminal domain of MerA; NosL, L protein from the nitrous oxide reductase (*nos*) operon; RMSD, root-mean-square deviation; SAD, single anomalous dispersion; TBT, tributyltin(IV) cation; TEL, triethyllead(IV) cation; TET, triethyltin(IV) cation; TML, trimethyllead(IV) cation; TMT, trimethyltin(IV) cation; TPT, triphenyltin(IV) cation; TTEL, tetraethyllead(IV); TTML, tetramethyllead(IV); UV−vis, ultraviolet−visible.

■ ASSOCIATED CONTENT

Supporting Information

The Supporting Information is available free of charge on the ACS Publications website at DOI: 10.1021/jacs.6b11327.

Binding of TML and DEL to MerB; fluorescence spectra of MerB with MeHg, DET, and DEL; binding of TMT to MerB; fluorescence spectra of MerB and TML with NMerA (PDF)

■ AUTHOR INFORMATION

Corresponding Author

*jg.omichinski@umontreal.ca

ORCID

Dean E. Wilcox: 0000-0003-2061-4838

James G. Omichinski: 0000-0002-3543-1914

Notes

The authors declare no competing financial interest.

■ ACKNOWLEDGMENTS

This work was supported by grants from the Natural Sciences and Engineering Research Council of Canada (NSERC) to J.G.O. and J.S. as well as from the National Science Foundation to D.E.W. (CHE-1308598). H.W. was supported by a grant from the Ministry of Higher Education and scientific research in Egypt (cultural affairs and missions sector). Research was carried out in part at the National Synchrotron Light Source, Brookhaven National Laboratory, which is supported by the U.S. Department of Energy, Division of Materials Sciences and Division of Chemical Sciences, under Contract No. DE-AC02-98CH10886 and the Canadian Light Source (CLS), which is supported by NSERC, the National Research Council Canada, the Canadian Institutes of Health Research, the Province of Saskatchewan, Western Economic Diversification Canada, and the University of Saskatchewan.

■ REFERENCES

(1) Miller, S. M. *Essays Biochem.* **1999**, *34*, 17−30.
(2) Jackson, W. J.; Summers, A. O. *J. Bacteriol.* **1982**, *151*, 962−970.
(3) Schottel, J.; Mandal, A.; Clark, D.; Silver, S.; Hedges, R. W. *Nature* **1974**, *251*, 335−7.
(4) Schottel, J. L. *J. Biol. Chem.* **1978**, *253*, 4341−4349.
(5) Barkay, T.; Miller, S. M.; Summers, A. O. *FEMS Microbiol. Rev.* **2003**, *27*, 355−384.
(6) Huang, C. C.; Narita, M.; Yamagata, T.; Endo, G. *Gene* **1999**, *239*, 361−6.
(7) Begley, T. P.; Walts, A. E.; Walsh, C. T. *Biochemistry* **1986**, *25*, 7186−92.
(8) Begley, T. P.; Walts, A. E.; Walsh, C. T. *Biochemistry* **1986**, *25*, 7192−200.
(9) Fox, B.; Walsh, C. T. *J. Biol. Chem.* **1982**, *257*, 2498−2503.

DOI: 10.1021/jacs.6b11327
J. Am. Chem. Soc. 2017, 139, 910−921

(10) Fox, B. S.; Walsh, C. T. *Biochemistry* **1983**, *22*, 4082−8.
(11) Omichinski, J. G. *Science* **2007**, *317*, 205−6.
(12) Benison, G. C.; Di Lello, P.; Shokes, J. E.; Cosper, N. J.; Scott, R. A.; Legault, P.; Omichinski, J. G. *Biochemistry* **2004**, *43*, 8333−8345.
(13) Hong, B. Y.; Nauss, R.; Harwood, I. M.; Miller, S. M. *Biochemistry* **2010**, *49*, 8187−8196.
(14) Hamlett, N. V.; Landale, E. C.; Davis, B. H.; Summers, A. O. *J. Bacteriol.* **1992**, *174*, 6377−85.
(15) Morby, A. P.; Hobman, J. L.; Brown, N. L. *Mol. Microbiol.* **1995**, *17*, 25−35.
(16) Schue, M.; Glendinning, K. J.; Hobman, J. L.; Brown, N. L. *BioMetals* **2008**, *21*, 107−16.
(17) Johs, A.; Harwood, I. M.; Parks, J. M.; Nauss, R. E.; Smith, J. C.; Liang, L.; Miller, S. M. *J. Mol. Biol.* **2011**, *413*, 639−56.
(18) Hong, L.; Sharp, M. A.; Poblete, S.; Biehl, R.; Zamponi, M.; Szekely, N.; Appavou, M. S.; Winkler, R. G.; Nauss, R. E.; Johs, A.; Parks, J. M.; Yi, Z.; Cheng, X.; Liang, L.; Ohl, M.; Miller, S. M.; Richter, D.; Gompper, G.; Smith, J. C. *Biophys. J.* **2014**, *107*, 393−400.
(19) Lafrance-Vanasse, J.; Lefebvre, M.; Di Lello, P.; Sygusch, J.; Omichinski, J. G. *J. Biol. Chem.* **2009**, *284*, 938−944.
(20) Parks, J. M.; Guo, H.; Momany, C.; Liang, L. Y.; Miller, S. M.; Summers, A. O.; Smith, J. C. *J. Am. Chem. Soc.* **2009**, *131*, 13278−13285.
(21) Bizily, S. P.; Rugh, C. L.; Summers, A. O.; Meagher, R. B. *Proc. Natl. Acad. Sci. U. S. A.* **1999**, *96*, 6808−13.
(22) Bizily, S. P.; Rugh, C. L.; Meagher, R. B. *Nat. Biotechnol.* **2000**, *18*, 213−7.
(23) Rugh, C. L.; Wilde, H. D.; Stack, N. M.; Thompson, D. M.; Summers, A. O.; Meagher, R. B. *Proc. Natl. Acad. Sci. U. S. A.* **1996**, *93*, 3182−7.
(24) Sigel, A.; Sigel, H.; Sigel, R. O., In *Organometallics in Environment and Toxicology*; RCS Publishing: Cambridge, U.K., 2010; Vol. 7.
(25) Dubalska, K.; Rutkowska, M.; Bajger-Nowak, G.; Konieczka, P.; Namieśnik, J. *Crit. Rev. Anal. Chem.* **2013**, *43*, 35−54.
(26) Graceli, J. B.; Sena, G. C.; Lopes, P. F. I.; Zamprogno, G. C.; da Costa, M. B.; Godoi, A. F. L.; dos Santos, D. M.; de Marchi, M. R. R.; dos Santos Fernandez, M. A. *Reprod. Toxicol.* **2013**, *36*, 40−52.
(27) Sousa, A. C. A.; Pastorinho, M. R.; Takahashi, S.; Tanabe, S. *Environ. Chem. Lett.* **2014**, *12*, 117−137.
(28) Lobinski, R.; Boutron, C. F.; Candelone, J. P.; Hong, S.; Szpunar-Lobinska, J.; Adams, F. C. *Environ. Sci. Technol.* **1994**, *28*, 1467−71.
(29) Mason, R. P.; Benoit, J. M. In *Organometallic Compounds in the Environment*; John Wiley & Sons: New York, 2003; pp 57−99.
(30) Sunday, A. O.; Alafara, B. A.; Oladele, O. G. *Chem. Spec. Bioavail.* **2012**, *24*, 216−226.
(31) Jarvie, A. W. P.; Markall, R. N.; Potter, H. R. *Environ. Res.* **1981**, *25* (2), 241−249.
(32) Ou, L.-T.; Thomas, J. E.; Jing, W. *Bull. Environ. Contam. Toxicol.* **1994**, *52*, 238−245.
(33) Mitchell, C. S.; Shear, M. S.; Bolla, K. I.; Schwartz, B. S. *J. Occup. Environ. Med.* **1996**, *38*, 372−8.
(34) Walsh, T. J.; Tilson, H. A. *Neurotoxicology* **1984**, *5*, 67−86.
(35) Nesci, S.; Ventrella, V.; Trombetti, F.; Pirini, M.; Pagliarani, A. *Toxicol. In Vitro* **2011**, *25*, 951−959.
(36) Ou, L. T.; Jing, W.; Thomas, J. E. *Environ. Toxicol. Chem.* **1995**, *14*, 545−551.
(37) Cruz, A.; Oliveira, V.; Baptista, I.; Almeida, A.; Cunha, A.; Suzuki, S.; Mendo, S. *Environ. Toxicol.* **2012**, *27*, 11−7.
(38) Walts, A. E.; Walsh, C. T. *J. Am. Chem. Soc.* **1988**, *110*, 1950−1953.
(39) Di Lello, P.; Benison, G. C.; Valafar, H.; Pitts, K. E.; Summers, A. O.; Legault, P.; Omichinski, J. G. *Biochemistry* **2004**, *43*, 8322−32.
(40) McCoy, A. J.; Grosse-Kunstleve, R. W.; Adams, P. D.; Winn, M. D.; Storoni, L. C.; Read, R. J. *J. Appl. Crystallogr.* **2007**, *40*, 658−674.
(41) Emsley, P.; Cowtan, K. *Acta Crystallogr., Sect. D: Biol. Crystallogr.* **2004**, *60*, 2126−32.
(42) Adams, P. D.; Afonine, P. V.; Bunkoczi, G.; Chen, V. B.; Davis, I. W.; Echols, N.; Headd, J. J.; Hung, L. W.; Kapral, G. J.; Grosse-Kunstleve, R. W.; McCoy, A. J.; Moriarty, N. W.; Oeffner, R.; Read, R. J.; Richardson, D. C.; Richardson, J. S.; Terwilliger, T. C.; Zwart, P. H. *Acta Crystallogr., Sect. D: Biol. Crystallogr.* **2010**, *66*, 213−21.
(43) Chen, V. B.; Arendall, W. B., 3rd; Headd, J. J.; Keedy, D. A.; Immormino, R. M.; Kapral, G. J.; Murray, L. W.; Richardson, J. S.; Richardson, D. C. *Acta Crystallogr., Sect. D: Biol. Crystallogr.* **2010**, *66*, 12−21.
(44) Eisler, R. *Lead Hazards to Fish, Wildlife, and Invertebrates: A Synoptic Review*; Report 14; Biological Report 85(1.14); U.S. Department of the Interior, Fish and Wildlife Service: Laurel, MD, 1988.
(45) Jarvie, A. W. P. *Sci. Total Environ.* **1988**, *73*, 121−126.
(46) Di Lello, P. D.; Lafrance-Vanasse, J.; Omichinski, J. G. The Organomercurial Lyase MerB. In *Handbook of Metalloproteins*; John Wiley & Sons: New York, 2006.
(47) Chien, M. F.; Narita, M.; Lin, K. H.; Matsui, K.; Huang, C. C.; Endo, G. *J. Biosc. Bioengineer.* **2010**, *110*, 94−8.
(48) Gupta, A.; Phung, L. T.; Chakravarty, L.; Silver, S. *J. Bacteriol.* **1999**, *181*, 7080−7086.
(49) Wang, Y.; Moore, M.; Levinson, H. S.; Silver, S.; Walsh, C.; Mahler, I. *J. Bacteriol.* **1989**, *171*, 83−92.
(50) Wahba, H. M.; Lecoq, L.; Stevenson, M.; Mansour, A.; Cappadocia, L.; Lafrance-Vanasse, J.; Wilkinson, K. J.; Sygusch, J.; Wilcox, D. E.; Omichinski, J. G. *Biochemistry* **2016**, *55*, 1070−1081.
(51) Weber, F.-A.; Voegelin, A.; Kaegi, R.; Kretzschmar, R. *Nat. Geosci.* **2009**, *2*, 267−271.

DOI: 10.1021/jacs.6b11327
J. Am. Chem. Soc. 2017, 139, 910−921